Focused ultrasound sensing in water using a GCLAD system

James N. Caron[1,2]

[1]*Research Support Instruments, 4325-B Forbes Boulevard, Lanham, MD 20706, USA*
[2]*Quarktet, 205 Indian Spring Drive, Silver Spring, MD 20901, USA*
Caron@RSImd.com

Abstract. Gas-coupled Laser Acoustic Detection (GCLAD) has been developed as a technique to sense airborne ultrasound waves by passing a laser beam through the acoustic disturbance. Fluctuations in the medium's index of refraction divert the beam from the original path. A position-sensitive photodetector receives the beam and senses the change created by the acousto-optic interaction. The method has proven to be a simple and effective method for sensing ultrasound that has been transmitted from materials and is suitable for applications in materials characterization and non-destructive evaluation.

By passing the laser beam through the glass windows of a water tank, the same method can be used for immersion detection of ultrasound. In this study, a 10 MHz immersed focused transducer was used to generate ultrasound in an immersed test sample. A laser beam is directed through the tank twice to capture the ultrasound before and after it passes through the material. The arrangement is used to directly compare the sensitivity of the immersed GCLAD arrangement with a commercial transducer. Ultrasound C-scans were created to produce individual spatial resolution measurements for the vertical and horizontal directions.

Introduction

Gas-coupled Laser Acoustic Detection (GCLAD) senses airborne ultrasound waves by passing a laser beam through the acoustic disturbance. [1] Fluctuations in the medium's index of refraction divert the beam from the original path. A position-sensitive photodetector receives the beam and senses the change created by the acousto-optic interaction. The method has proven to be a simple and effective method for sensing airborne ultrasound transmitted from materials and is suitable for materials characterization and non-destructive evaluation (NDE).

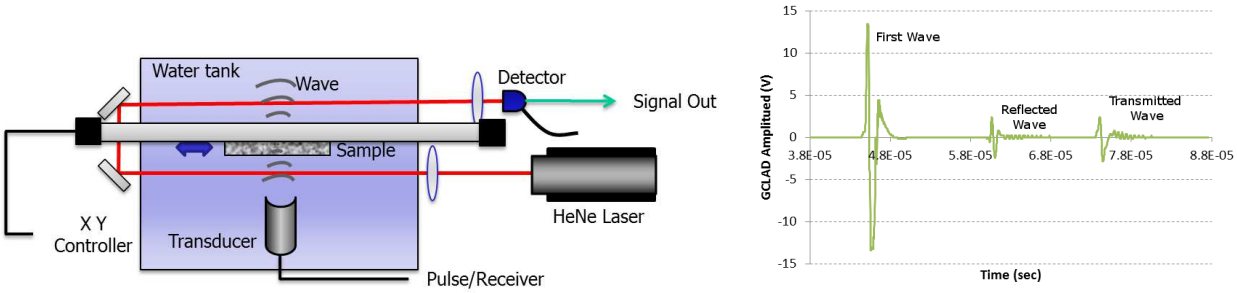

FIGURE 1. (Left) Schematic for underwater detection of ultrasound using GCLAD. An immersed ultrasound transducer delivers an ultrasonic wave to the sample. The optical beam passes in front of and behind the sample to sense waveform at different points. A position-sensitive photodetector senses the deflection of the beam created by the passing waveform. (Right) A waveform averaged from 64 triggers as sensed using GCLAD. The sample is a 2 mm thick aluminum plate. The first peak, which is clipped on the current scale, represents the direct wave while the second peak results from reflection from the plate surface. The third peak is from transmission through the sample. The following ripples are from multiple internal reflections of the wave.

This paper continues the study of GCLAD, but using water as the medium. [2] providing improved sensitivity and detection of higher frequencies. [3] Ultrasound detection in water by laser beam has been reported before, [4, 5]

FIGURE 2. Ultrasound C-scans for a 2.0 mm thick aluminum plate from the first wave (left), reflected wave (middle) and transmitted wave (right). The presence of tape on the reverse side of the plate improves plate-to-water coupling producing slightly higher amplitudes.

but not as a means for NDE. A primary objective of this study is to determine the situations where this technique may complement or supplant traditional immersion transducers.

The experimental setup is shown in Figure 1 (left). An intensity-stabilized 4.5 mW Spectra-Physics HeNe laser is directed through the tank, passing about 1 cm in front of the sample, and redirected into the tank by two turning mirrors. The beam passes 1 cm behind the sample and out of the tank. The first convex lens, with focal length of 75 mm, focuses the beam near the interaction point and the second convex lens focuses the beam to just beyond the photocell for best sensitivity. [6]

By passing the beam through the tank twice, the ultrasound can be sensed before and after transmission through the sample within a single trigger event. In a typical waveform, shown in Figure 1 (right), the first peak was produced by direct route from the transducer. The second was produced by the reflection from the sample surface while the third peak resulted from the transmission of the wave through the sample. Ripples following the second and third peaks stem from internal reflections in the sample.

Signal Strength

The immersed transducer can also be used to sense the reflected ultrasound allowing for a direct comparison to the GCLAD signal. The signal-to-noise ratio (SNR) of a reflected wave for a single trigger event was measured as 85.5 for the transducer and 42.3 for the GCLAD sensor. GCLAD SNR can be significantly increased, if needed, with improved detector electronics and increased laser power. [7] For example, replacing the current laser with a low-noise 200 mW laser would increase the SNR by a factor of 6.7.

The frequency response of GCLAD depends on the ratio of the beam size at the interaction point and the acoustic wavelength. If the wavelength is similar or smaller than the laser beam width, the beam will be simultaneously refracted in different directions by different portions of the wave. In the present case, the wavelength is 0.15 mm for a 10 MHz wave and 1.5 mm for a 1 MHz wave in water. The laser beam has a diameter of 0.5 mm when leaving the laser and a divergence of 1.8 mrad. As a result of the first convex lens, the spot size at the interaction point was calculated to be 0.24 mm. While this value is larger than the wavelength, small misalignments to the beam position can reveal the higher frequency components.

Ultrasound C-Scans

The C-scanning system, depicted in the figure 1, consists of two screw-driven arms operated by a Velmex VP9000 controller. For each position, a full waveform from a single trigger event is recorded. Post processing consists of identifying the peaks of interest and recording their amplitudes as a function of position. Figure 2 shows three images created from a 128 by 128 pixel C-scan of a 2.0 mm thick aluminum panel. The step size was 0.095 mm producing a 1.22 by 1.22 cm^2 scan area. A square-shaped piece of transparent tape was placed on the back-side of the panel to provide a feature. The left image is from the first wave and can be used for correcting the ultrasound images for variations in signal. The middle image is measured from the peak-to-peak amplitudes of the reflected wave, showing a very consistent amplitude across the sample. The right image was produced from the transmitted

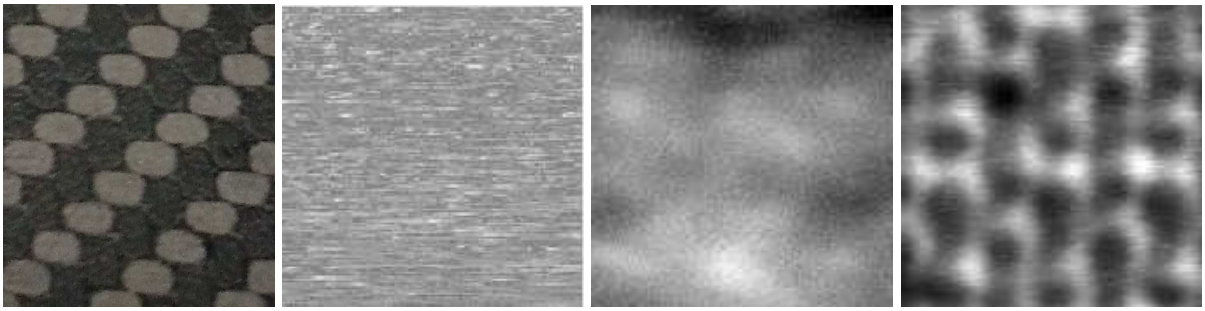

FIGURE 3. The far left optical image the approximate C-scan size for a 0.56 mm thick composite panel. The following images show the first wave (left middle), reflected (right middle), and transmitted wave (far right).

waves and reveals the presence of the tape. Values in the image range from 4.2 to 5 volts, well above the noise floor of 0.058 volts.

Figure 3 shows the same scan performed on a 0.56 mm thick graphite reinforced composite panel with no known defects. An optical image of the approximate scanned area is on the left. The second image was derived from the peak-to-peak amplitudes of the first wave. The third image is derived from the reflected wave. With the thinness of this sample, this waveform is a combination of reflection from the sample surface and the interior. The last image is the transmission wave component and reveals the inner structure of the sample.

Scan Resolution

The spatial resolution for a focused transducer is limited by the ultrasound beam diameter at focus. The expected waist size of a focused transducer is calculated using $w \approx \frac{\lambda f}{D}$ where λ is the acoustic wavelength for the medium, f is focal length of the transducer, and D is the aperture diameter. [8] For a 10 MHz transducer, diameter of 13 mm, and focal length of 76 mm, we can expect the beam size on the sample to be 0.87 mm. To measure resolution, an edge feature was created on a 2.0 mm thick aluminum plate by placing electrical tape diagonally across the sample, as shown in Figure 4 (left). A 128 by 124 pixel C-scan was created on a region of 4.07 by 3.94 cm^2. Figure 4 (middle) shows the transmission signal, revealing the feature. The presence of the tape reduced the average amplitude of the transmitted wave by 27 %. The source of the dip before the tape has not been determined yet, but it does not adversely affect the analysis here.

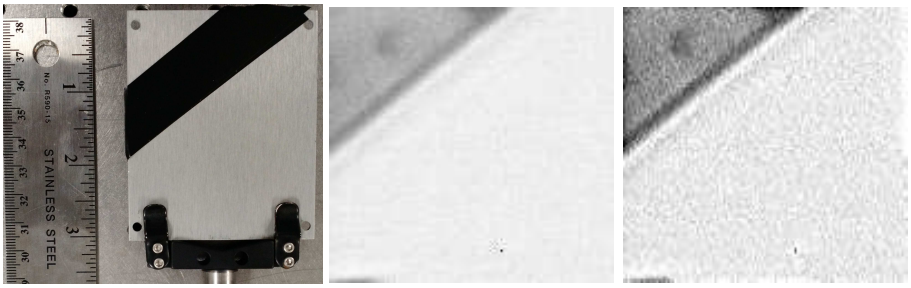

FIGURE 4. The left image is an optical image showing the position of black tape placed diagonally on a 2.0 mm thick aluminum plate. The middle image is a 128 by 124 pixel C-scan across the feature while recording the transmitted peak amplitudes. A deconvolution is shown on the right.

To determine resolution, nine line-outs were taken from the region defined by pixels [14,22] to [81,31]. As each row has the edge is a different position, the location of the edge is determined by fitting each row to the equation

$$F(x) = A_0 + A_1 \left[1 - \frac{1}{1 + \exp\left(-A_3 * (x - A_2)\right)} \right] \tag{1}$$

based on a sigmoid function. Each row of data is aligned to the A_2 edge position. These values are combined into a single data set, sorted, and fitted again to the sigmoid function. The data and fit plotted are shown in Figure 5.

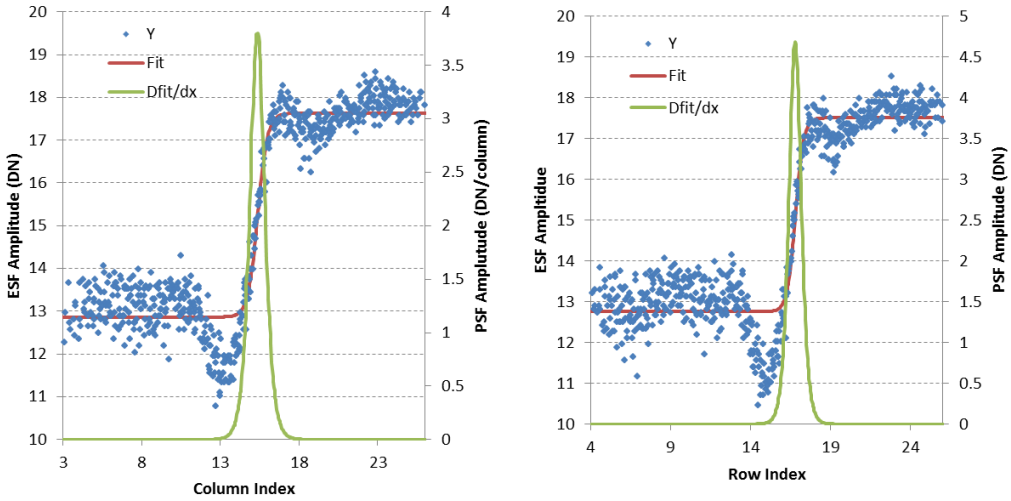

FIGURE 5. (Left) Edge response function (Y), sigmoid fit, and derivative for the horizontal direction. Right Edge response function (Y), sigmoid fit, and derivative for the vertical direction.

The process is repeated on the columns by rotating the image 90 degrees and operating on the area defined by [14,106] to [81,115]. The derivative of the fit produces a measure of the resolution of the system. Using the full width at half maximum (FWHM), the resolution was calculated to 1.06 mm in the horizontal direction and 0.818 mm for the vertical direction. The resolution in the direction parallel to the laser beam is larger than in the perpendicular direction, but not significantly so. The horizontal direction exceeds the waist size by 0.19 mm whereas the vertical resolution is better by 0.052 mm.

With images of sufficient SNR, deconvolution methods can be used to improve the resolution. To this end, we apply an approximation of the SeDDaRA approach [9], Figure 4 (right), to determine and remove the point spread function. With deconvolution, the FWHM in the horizontal direction falls to 0.58 mm and 0.47 mm in the vertical direction. Since the success of the deconvolution is limited by noise level, improvements in the SNR of the system, accomplished by using a higher power laser or signal averaging may provide additional improvements.

REFERENCES

[1] J.N. Caron, Y. Yang, J.B. Mehl, and K.V. Steiner, "Gas coupled laser acoustic detection for ultrasound inspection of composite materials," *Materials Evaluation*, **58**, No. 5, p. 667, (2001).

[2] J.N. Caron, and P. Kunapareddy, "Application of gas-coupled laser acoustic detection to gelatins and underwater sensing," In *Review of Progress in Quantitative Nondestructive Evaluation*, AIP Publishing, **1581**, no. 1, p. 458, (2014).

[3] J.N. Caron, and G. P. DiComo, "Frequency response of optical beam deflection by ultrasound in water," *Applied optics* **53**, no. 32, p. 7677, (2014).

[4] P.-K. Choi, "Broadband measurements of ultrasonic waves using optical beam deflection," in AIP Conference Proceedings, **524**, p. 325, (2000).

[5] P. Gregorčič and J. Možina, "A beam-deflection probe as a method for optodynamic measurements of cavitation bubble oscillations," *Meas. Sci. Technol.* **18**, p. 2972 (2007).

[6] J.N. Caron, "Displacement and deflection of an optical beam by airborne ultrasound," *Review Of Progress In Quantitative Nondestructive Evaluation*, D. O. Thompson, and D. E. Chimenti, eds., (AIP Conference Proceedings), **975**, No. 1, p. 247, (2008).

[7] Caron, James N., James B. Mehl, and Karl V. Steiner, "Progress in Gas-Coupled Laser Acoustic Detection for NDE Applications," *Review of Progress in Quantitative Nondestructive Evaluation*. Springer US, p. 317 (1999).

[8] A. Ng and J. Swanevelder, "Resolution in ultrasound imaging," *Continuing Education in Anaesthesia, Critical Care and Pain* **11**, no. 5, p. 186, (2011).

[9] J. N. Caron, N. M. Namazi, and C. J. Rollins, "Noniterative blind data restoration by use of an extracted filter function," *Appl. Opt.* **32**, p. 6884, (2002).